FUSE In-Orbit Attitude Control with Two Reaction Wheels and No Gyroscopes

Jeffrey W. Kruk[a], Brian F. Class[b], Dan Rovner[b], Jason Westphal[b], Thomas B. Ake[a], H. Warren Moos[a], Bryce Roberts[a], and Landis Fisher[a]

[a]Dept. of Physics and Astronomy, The Johns Hopkins University, 3400 N. Charles St., Baltimore, MD, 21218 USA
[b]Orbital Sciences Corp., 21839 Atlantic Blvd., Dulles, VA, 20166 USA

ABSTRACT

The Far Ultraviolet Spectroscopic Explorer is a NASA Origins mission launched in June 1999 to obtain high-resolution spectra of astronomical sources at far-ultraviolet wavelengths. The science objectives require the satellite to provide inertial pointing at arbitrary positions on the sky with sub-arcsecond accuracy and stability. The requirements were met using a combination of ring-laser gyroscopes, three-axis magnetometers, and a fine error sensor for attitude knowledge, and reaction wheels for attitude control. Magnetic torquer bars are used for momentum management of the reaction wheels, and coarse sun sensors for safe mode pointing.

The gyroscopes are packaged as two coaligned inertial reference units of three orthogonal gyroscopes each. There are four reaction wheels: three oriented along orthogonal axes, the fourth skewed at equal angles (54.7°) with respect to the others. Early in the mission the gyroscopes began showing signs of aging more rapidly than expected, and one failed after two years of operation. In addition, two of the orthogonal wheels failed in late 2001. The flight software has been modified to employ the torquer bars in conjunction with the two remaining wheels to provide fine pointing control. Additional new flight software is under development to provide attitude control if both gyroscopes fail on one or more axes. Simulations indicate that the pointing requirements will still be met, though with some decrease in observing efficiency. We will describe the new attitude control system, compare performance characteristics before and after the reaction wheel failures, and present predicted performance without gyroscopes.

Keywords: FUSE, Satellites, Attitude Control

1. INTRODUCTION

The Far Ultraviolet Spectroscopic Explorer (FUSE) is a NASA Origins mission launched in June 1999 to obtain high-resolution spectra of astronomical sources at far-ultraviolet wavelengths.[1] The science payload is a single instrument comprising four coaligned telescopes and prime-focus spectrographs.[2] The FUSE mission was originally approved for three years of science operations, and four additional years of extended mission operations have been approved. A current overview of FUSE operations is given in Reference 3.

The science objectives of the mission impose a number of requirements on the spacecraft attitude control system. The spacecraft must provide three-axis stabilized inertial pointing of the telescopes at astronomical sources located at arbitrary positions on the sky, subject to solar avoidance constraints. The pointing stability must be better than $0.5''$, 1σ, and the absolute pointing accuracy requirement is $1''$. Large attitude maneuvers (slews) have a peak rate of 4° per minute (a compromise between operational efficiency and the time needed to close the telescope doors in response to detection of a dangerously bright object), and a relative accuracy of $10'$. Small slews have an accuracy requirement of $3''$. Finally, the spacecraft must be able to slew slowly so as to track moving objects such as planets or comets.

The FUSE orbit is circular, with an altitude of $\sim$767 km and inclination of 25°. Therefore, the line of sight to most targets will be occulted by the Earth for roughly half of each orbital period. Most observations last longer than one orbit, so observational efficiency requires that the time required to point the telescopes accurately towards the target (the "target acquisition") must be a small fraction of the orbit. There is a small region, roughly 22° in diameter, centered on the pole

Send correspondence to J.W.K. E-mail: kruk@pha.jhu.edu

of the orbit that is far enough from the Earth limb to be observable continuously throughout the orbit. The plane of the orbit precesses by 6° per day, so the pole of the orbit sweeps a complete circle around the celestial pole with a period of 60 days.

In this paper we will describe the original design of the attitude control system (section 2), changes resulting from the loss of two of the reaction wheels (section 3), and modifications in progress to operate in the event of gyroscope failures in any or all axes (section 4).

2. ORIGINAL ACS DESIGN

The FUSE attitude control system (ACS) was designed to be a fully-redundant three-axis stabilized system with zero net angular momentum. Three-axis magnetometers and coarse sun sensors provide attitude information, and ring-laser gyroscopes provide rate measurements. Fine pointing is achieved using a Fine Error Sensor (FES) that views the sky through the instrument optics. The attitude estimate is propagated using the gyro data and continuously corrected by a Kalman filter. All functions other than those associated with the FES and observation sequencing are performed by a dedicated ACS processor located in the spacecraft bus. Reaction wheel assemblies (RWAs) provide attitude control, and magnetic torquer bars are used to maintain the average wheel momenta near pre-set bias levels.

A schematic view of the satellite and the coordinate axes used by the ACS are shown in Figure 1. The thermal and power systems were designed assuming that only the –X and –Z sides of the satellite would be directly illuminated by the sun. For most operations this imposes a constraint on the spacecraft roll of $\pm 15°$, though roll angles up to $\pm 45°$ are allowed for limited periods (zero roll corresponds to the sun lying in the X-Z plane). The solar arrays rotate about the pitch axis to maintain their orientation normal to the sun. The pitch axis rotation determines the angle of the telescope boresight with respect to the sun. The boresight is never allowed within 45° of the sun, but thermal effects on instrument alignment are such that observations are rarely scheduled with the boresight closer than 90° to the sun. There are no constraints on the yaw orientation. The FUSE satellite mass is ~ 1320 kg, of which roughly 40% is contained within the spacecraft bus, and the total satellite length is ~ 5.5 m.

2.1. Hardware Resources: Sensors

Redundant three-axis magnetometers (TAMs) are mounted on the boom supporting the S-band omni antenna on the +X (shadowed) side of the satellite. TAM measurements are sampled at 5 Hz; samples that overlap switching transients in the torquer bars are discarded. The TAM calibration provides measurements of the spacecraft attitude relative to the instantaneous geomagnetic field vector ($\vec{\mathbf{B}}$) that are accurate to about 1°. This information can be combined with knowledge of the orbital elements and a model of the Earth's $\vec{\mathbf{B}}$-field to determine the attitude in inertial space. Note that the TAMs provide no information on the rotation of the spacecraft around the instantaneous $\vec{\mathbf{B}}$ direction. However, the direction of the $\vec{\mathbf{B}}$-field changes fairly rapidly as the spacecraft moves around the orbit. Therefore, if the spacecraft is being held inertially fixed by means of data obtained from the gyroscopes or FES, it is possible to accumulate accurate attitude information from the TAMs for all three axes over a reasonable period of time.

There are two redundant inertial reference units (IRUs), each consisting of a set of three ring-laser gyroscopes mounted orthogonally and aligned to the spacecraft body axes. The IRU measurements of accumulated angular motion are sampled at 25 Hz and filtered. The software can combine data from any axis of both units simultaneously, although only a single unit is powered during normal operations.

The coarse sun sensors (CSSs) are mounted on the corners of the solar arrays, and provide a measure of the angle between the normal of the arrays and the sun. This measurement is accurate to about 7°, limited in part by the errors introduced by Earth's albedo, and saturates at 25°. They provide no information, of course, while the spacecraft is on the night side of the Earth.

The redundant FES system[4] is an integral part of the telescope optical system. The FES is a CCD camera that reimages the telescope focal plane, with a field of view approximately $19'$ square. It can provide either full field of view images or centroided positions of selected guide stars. FES data are available only when the line of sight to the target is not occulted by the Earth. The image and centroid data are transferred over a MIL-STD-1553 bus for processing by the Instrument Data System[5] (IDS).

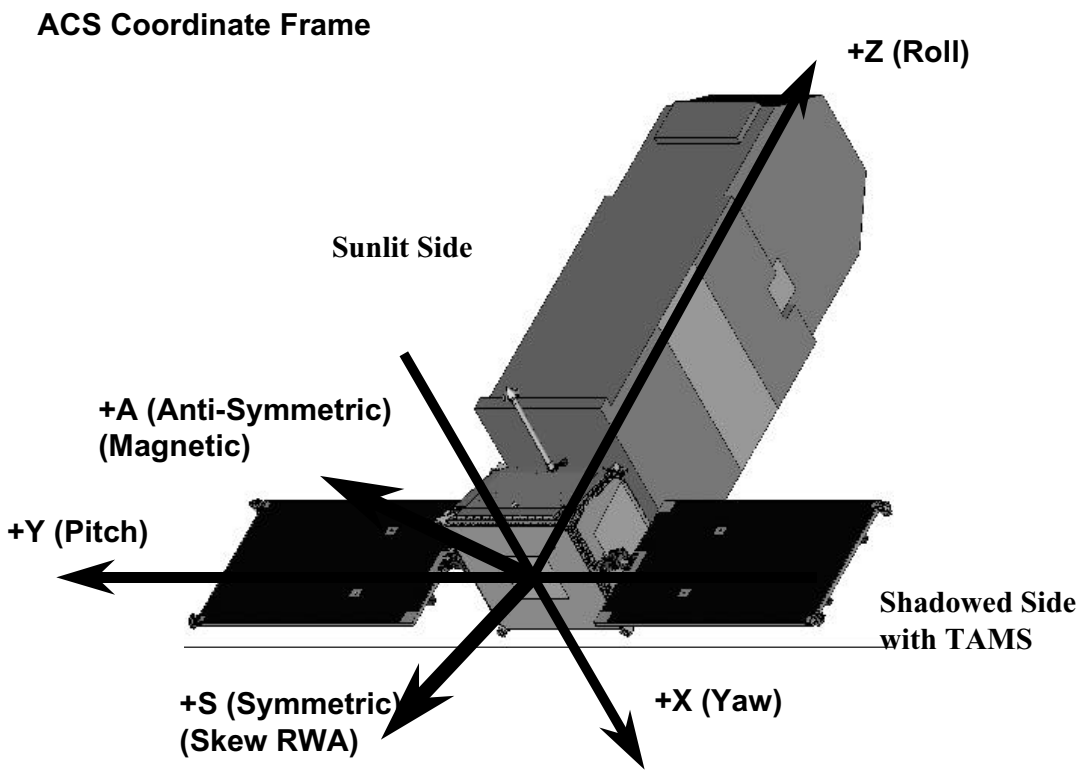

Figure 1. The FUSE coordinate axes are shown overplotted on a schematic layout of the satellite. The spacecraft bus is mounted under the science instrument. The line-of-sight of the four co-aligned telescopes is along the +Z axis. The –X side of the satellite is always oriented towards the sun, so that the instrument radiators mounted on the side panels have at most grazing illumination by sunlight. The solar panels rotate about the Y-axis to maintain a near-90° orientation to the sun. The S-axis is the projection of the skew-wheel axis onto the X-Y plane, and the A-axis is controlled solely by magnetic torque following the failures of the X and Y reaction wheels.

2.2. Hardware Resources: Actuators

The reaction wheel assemblies are used for all direct control of the satellite attitude. Three wheels are mounted orthogonally, aligned with the spacecraft body axes. A fourth, redundant, wheel is mounted skewed at equal angles (54.7°) to each of the body axes, aligned diagonally in the +X, +Y, +Z quadrant. This "skew" wheel could be used to provide control about any of the other axes if one of the orthogonal wheels were to fail. In normal "4-wheel" operations, the skew wheel was biased at a fixed momentum, and the other three wheels were biased in the opposite direction to maintain zero net angular momentum while keeping the speed of each wheel away from zero (which prevented the slightly degraded pointing performance associated with zero wheel speed crossings). The RWAs each provide torque up to 55 milli-Newton-meters (m-Nm), with a resolution of 0.027 m-Nm and a peak momentum storage of 21 Nms.

Magnetic torquer bars (MTBs) provide momentum management of the RWAs. The three MTBs are mounted orthogonally, each parallel to one of the body axes. The RWAs provide fine control of the satellite attitude by exchanging momentum between the satellite and the wheels, but cannot exert torques on the external environment. External torques (primarily gravity gradient) do not generally average to zero over time, and would cause the wheels to speed up to saturation in a relatively small number of orbits. The MTBs are driven continuously to exert torques against the Earth's $\vec{\mathbf{B}}$-field so as to maintain each wheel near its preset bias speed. The net dipole created by energizing the three MTBs is controlled by selecting the polarity of each MTB and controlling the time-averaged current by pulse-width modulation with a 10-second command period and 200 millisecond minimum pulse width.

2.3. Operations

Overall control of science activities and fine-pointing determination is provided by the instrument computer, the IDS. All commands needed for slewing the spacecraft to a new target, performing target acquistions, and obtaining science data are loaded into the IDS in the form of scripts written in the Spacecraft Command Language. The command load for each observation includes a catalog of up to 200 stars that spans a field roughly 1° in diameter centered on the target. The main steps in a target acquisition sequence are as follows:

1. The FES obtains a full FOV image and transfers it to the IDS.
2. The IDS processes the image and determines locations of up to 30 stars.
3. The IDS commands the FES to centroid 3 to 6 of the brightest stars at 1 Hz, computes quaternions, and transmits them to the ACS. These quaternions are flagged as "unknown", because the stars have not yet been identified. These data are used to maintain a fixed spacecraft attitude while the absolute attitude is determined from the FES image.
4. The IDS compares the objects in the image to the star catalog uplinked for this observation and determines the absolute attitude.
5. The IDS sends the absolute quaternion to the ACS, which initiates a slew to remove the residual attitude error.
6. The IDS commands the FES to centroid pre-selected stars surrounding the target, computes quaternions, and sends them to the ACS for input to the Kalman filter.

The architecture of the observation scripting system is described in greater detail in Reference 6. The quaternions computed by the combined IDS/FES system have a relative accuracy better than $0.2''$ (for guidestars at the FES limiting sensitivty of V=13.5 or brighter); the absolute accuracy is limited by uncertainties in the tabulated guide star positions, but is typically about $0.5''$.

The division of functions between the ACS, IDS, and FES provided the performance necessary to meet mission requirements and resulted in simple interfaces that facilitated rapid development and integration of the subsystems prior to launch. However, another consequence of this partitioning is that the performance of the different subsystems are interdependent. Two particular areas where this affects the design of the zero-gyro system are mentioned briefly here, and will be discussed in greater detail in subsequent sections. First, the transfer of the FES image to the IDS is limited by the speed of the 1553 bus. As a result, the time interval between obtaining the initial FES image and the command to the FES selecting regions to be centroided ranges from about 25 seconds to as much as 60 seconds, depending primarily on the binning of the image. It is essential that the ACS limits attitude drift during this time to at most a few arcseconds, which is easily achieved when using gyro data. Otherwise, the intended guide stars will not be present in the regions being centroided and the acquisition will fail. Second, there is presently a mismatch between the accuracy of the attitude that can be derived solely from the TAMs (about 1° in radius, assuming accurate rate sensing is available from another sensor, such as the gyroscopes), and the size of the star catalog uplinked for each observation (about 0.5° radius). If data from the FES have been available to the ACS within the past two or three orbits, the gyro drift bias estimate will be accurate and absolute attitude errors will be less than 0.5°. However, if the time interval without FES data exceeds 3 orbits, the attitude errors increase until they become limited by the accuracy of the TAMs; as a result it is often not possible to match stars in the FES images to the on-board catalog. In this case, the attitude determination must be performed on the ground using a larger star table. This is acceptable for recovery from occasional contingencies, but not for routine operations.

2.4. Performance

Performance of the original system was excellent. Absolute pointing accuracy was typically better than $1''$, and pointing jitter was typically about $0.35''$ RMS. Target acquisitions were quite efficient: for simple cases in which an isolated target was placed in the large spectrograph aperture, the acquisition would ordinarily take no more than 200 seconds. Allowing for settle time after the initial slew to a field would add less than 300 seconds in most cases. More complex acquisitions requiring offsets or peakups in one of the narrow spectrograph apertures would require several hundred seconds of additional time, but even the most complex acquisitions still left the majority of the visibility period in each orbit for obtaining science data. The overall performance of this system is described in more detail in Reference 7.

3. REACTION WHEEL FAILURES: MAGNETIC TORQUER BAR CONTROL

On August 4, 2000 the ACS flight software shut down the pitch-axis reaction wheel in response to an increase in drag in the wheel. Analysis by the vendor indicated that the likely cause was the growth of small bubbles in Kapton tape used to line the inner housing of the assembly. The RWA was designed to maintain a very close tolerance gap between the rotor and the housing, and the housing was lined with Kapton tape so that loads induced by launch vibrations would be absorbed by the tape rather than the rotor bearings. When the wheel was restarted, above-normal drag was present for several minutes but eventually disappeared. This was attributed to a gradual wearing-away of the Kapton that was in contact with the rotor, consistent with the tape-bubble hypothesis. This event is described in detail in Reference 8.

The yaw wheel experienced a similar shutdown on February 16, 2001. It too was returned to service, but nearly three days of operation were required before the increased drag had disappeared entirely.

The yaw wheel then experienced a more severe failure on November 25, 2001, stopping completely from increased drag even before the flight software monitoring the wheel initiated a shutdown. Unlike the previous events, attempts to restart the wheel did not result in any detectable motion. Operations continued normally in three-wheel mode, with the skew wheel providing yaw-axis control.

Finally, the pitch wheel also suffered a complete failure, stopping abruptly on December 10, 2001. It too has not moved despite repeated attempts to restart it. At this point the skew wheel was reconfigured to control the pitch axis, leaving the yaw axis uncontrolled. The spacecraft Z-axis was oriented perpendicular to the sun vector and the solar array normal aligned parallel to the sun vector, so that rotations about the yaw axis would leave the array normal pointed at the sun.

Crude control was restored to the yaw axis by means of a code patch uplinked to the ACS flight software on December 20, 2001. This patch redirected the yaw wheel torque requests to the wheel unloading routine, where they were added to the wheel unloading torque commands to the MTBs. This stabilized the attitude but did not permit fine control: use of the skew wheel to control pitch also applied torques about the other axes that were too large to be immediately counteracted by the much weaker MTBs. The result was that the yaw axis could only be controlled to a few degrees. At this point the satellite was slewed to point towards the orbit normal, an orientation in which gravity-gradient torques are minimized.

A more extensive modification of the control algorithm was then prepared. The first step was to decouple torques applied by the skew and roll wheels from torques required from the MTBs. This was accomplished by a redefinition of the control system coordinate axes: a 45° rotation about the Z axis replaced the pitch (Y) and yaw (X) axes with the new "symmetric" (S) and "anti-symmetric" A axes

$$\hat{\mathbf{S}} = \frac{1}{\sqrt{2}}(\hat{\mathbf{Y}} + \hat{\mathbf{X}}), \quad \hat{\mathbf{A}} = \frac{1}{\sqrt{2}}(\hat{\mathbf{Y}} - \hat{\mathbf{X}}). \tag{1}$$

The new S axis corresponds to the projection of the skew wheel momentum vector onto the X-Y plane in the +X+Y quadrant (hence the name symmetric); torques required about the S-axis can be supplied by the skew wheel with no coupling into the A-axis. The skew wheel coupling to the Z axis is easily handled by the roll wheel. Torques required about the A axis are supplied purely by the MTBs.

The MTB control software was also modified. The wheel unloading torques for the S and Z axes were combined with the control torque needed for the A axis to construct the required magnetic dipole, giving precedence to the control torque over the unload torque. The gains and limits of the A-axis controller were adjusted to accommodate the torque available from the MTBs. Additionally, the MTB pulse-width-modulation period was changed to three seconds to allow for a higher bandwidth controller and thus maintain fine pointing.

This new software was uploaded on January 24, 2002. Fine pointing control was established within minutes of the activation of the new code. Following a few days of initial checkout, science observations were interspersed with characterization and testing of the new controller, and full-time science operations resumed by the end of February.

The wheel failures have been ascribed, by the wheel vendor, to thermally induced distortions of the housing that resulted in contact with the rotor. The two remaining wheels are in a more benign thermal environment and are mounted differently, and are therefore considered much less likely to fail.

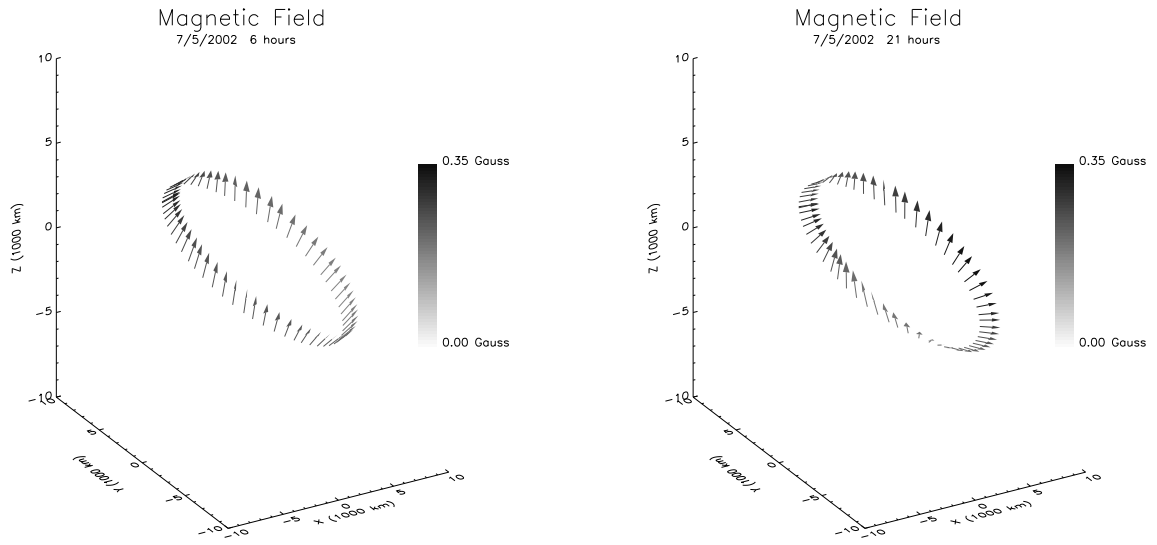

Figure 2. The magnetic field orientation is shown as a function of position around the FUSE orbit, for two orbits separated by about 15 hours. The field strength may vary by as much as a factor of two from one side of the orbit to the other. For some orbits, as in the left panel, the field direction changes by only a modest amount. Most orbits, however, are similar to the right panel in character, in that the field direction changes by 90° or more in a quarter-orbit. The coordinate axes indicate the position of FUSE in Earth-centered inertial coordinates.

Many aspects of system performance are affected slightly or not at all by use of MTBs in place of the two failed reaction wheels. Slew accuracy and absolute pointing accuracy are driven by gyro and FES performance, and are completely unaffected. Pointing jitter in the S and Z axes is also unaffected. Pointing jitter in the A-axis is roughly double what was obtained before, or about $0.7''$ RMS; this does not have a measureable effect on the science data. There is also a slowly-varying component to the A-axis pointing error that has a period of about half an orbit. The amplitude of this error depends on the angle of the line of sight to the orbit pole, ranging from zero near the pole to as much as $12''$at worst-case pole angles near 45°. This variation is comparable in magnitude and timescale to thermally-induced misalignments in the telescope optics that are corrected by the data calibration software; additional software to correct the science data for this pointing error has already been developed and is under test. We also expect that this pointing error can be greatly reduced by tuning the A-axis controller; analysis of the required parameter changes has been performed and uplink of the new values is expected in the near future.

Two aspects of pointing performance that have been significantly affected by the loss of the two wheels are slew speed and sky coverage. The geomagnetic field varies considerably in direction and strength depending on the position of FUSE in the orbit and the orientation of the orbit plane, as is shown in Figure 2. Even when the $\vec{\mathbf{B}}$ orientation is favorable, the maximum torque available from the MTBs is in the range of 2.5 m-Nm to 6.5 m-Nm, or roughly one-tenth of that provided by the RWAs. When the $\vec{\mathbf{B}}$-field is roughly parallel to the A-axis, no torque at all can be generated.

The dominant external disturbance is gravity-gradient torque acting on the satellite. This torque acts to align the satellite Z axis with the local zenith/nadir vector, and can be expressed as

$$\mathbf{N}_{GG} = \frac{3\mathrm{GM}_{\oplus}}{R^3}\ \hat{\mathbf{R}} \times (\mathbf{I}\hat{\mathbf{R}}) \tag{2}$$

where $\hat{\mathbf{R}}$ is the vector from the center of the Earth to the FUSE center of mass, $\mathrm{M}_{\oplus}$ is the mass of the Earth, G is Newton's constant, and $\mathbf{I}$ is the moment of inertia tensor of FUSE. If the off-diagonal terms of the inertia tensor are ignored (a roughly 1% effect), then this reduces to (all quantities expressed in spacecraft body axes):

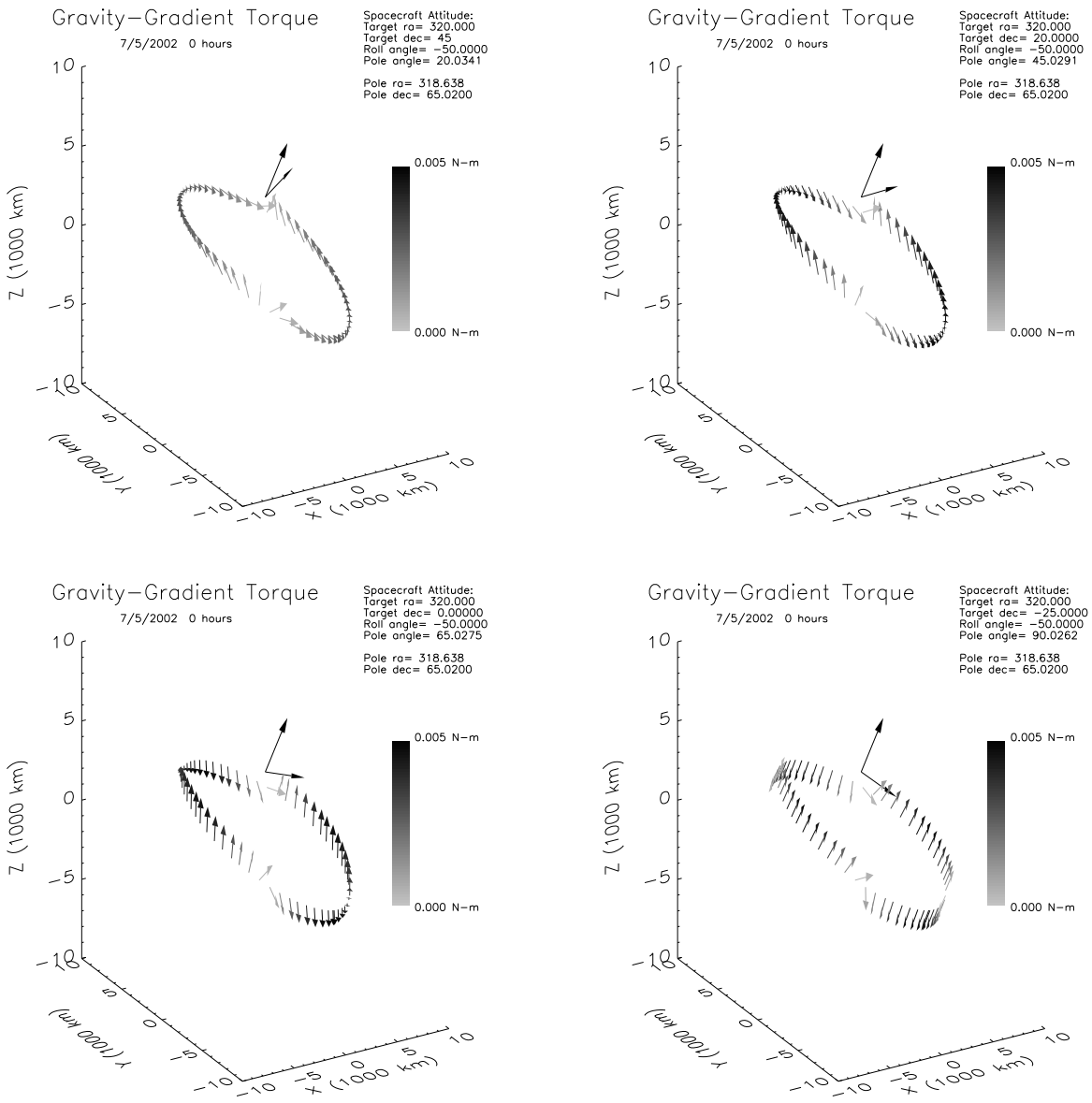

Figure 3. The gravity-gradient torque is shown as a function of position around the FUSE orbit for four different angles between the line of sight and the orbit pole. The longer arrow indicates the direction of the orbit normal and the shorter arrow indicates the direction of the line of sight. For small pole angles, the torque vector lies close to the tangent to the orbit and has relatively small magnitude (about 2.5 m-Nm for the 20° pole angle case in the upper left panel). As the pole angle increases the torque increases and the vector twists out of the orbit plane and changes direction more rapidly. At pole angles of 90° it is almost purely perpendicular to the plane.

$$\mathbf{N}_{GG} = \frac{3\mathrm{GM}_{\oplus}}{R^3}\left\{r_y r_z (I_{zz} - I_{yy})\hat{\mathbf{X}} + r_x r_z (I_{xx} - I_{zz})\hat{\mathbf{Y}} + r_x r_y (I_{yy} - I_{xx})\hat{\mathbf{Z}}\right\}, \tag{3}$$

where r_x, r_y, and r_z are the components of $\hat{\mathbf{R}}$ in spacecraft body axes.

The peak torques are $\sim$5 m-Nm, and occur at orientations of the Z-axis of 45° or more from the orbit pole. The behavior of the gravity-gradient torques as a function of orbit-pole angle is shown in Figure 3. At small pole angles,

the torque vector is primarily tangent to the orbit trajectory. As the pole angle of the line of sight increases the torque vector lifts further out of the orbit plane and twists about the orbit tangent more rapidly. When the line of sight lies in the orbit plane, the torque vector is normal to the plane and changes sign abruptly four times around the orbit (when the Z-axis is either parallel or perpendicular to the radius vector). The peak torque around the orbit is near zero when the line of sight is parallel to the orbit normal and increases with pole angle until it reaches a maximum of just over 5 m-Nm at a pole angle of 45°; at higher pole angles the peak torque remains at 5 m-Nm but changes direction more rapidly. This peak disturbance torque is comparable to the maximum torque available from the MTBs under the most favorable circumstances, indicating that careful planning is required to achieve continuous fine attitude control of the satellite at all attitudes. The rapid changes in orientation of both the $\vec{\mathbf{B}}$-field and gravity-gradient torque make this a challenging problem.

3.1. Mission Planning

Determining when a desired observation is possible is a complex task. The gravity-gradient disturbance torques can vary significantly in both magnitude and direction with the position of FUSE in its orbit, and depend also on the angle between the line of sight to the target and the normal to the orbital plane (which can change by as much as 50° over the 60-day orbit precession period). The spacecraft roll angle is constrained by needing to maintain the sun close to the X-Z plane, hence the orientation of the A-axis relative to the disturbance torques may only be varied slightly on any given day for a given astronomical target.

The available control torque depends on the $\vec{\mathbf{B}}$-field, but, as described in the previous section, the $\vec{\mathbf{B}}$-field varies greatly in both strength and direction as FUSE orbits the Earth. The Earth's field is a tilted, off-center dipole, with an inclination of about 11° with respect to the geographic axis, so the dipole axis sweeps out a 22° cone over 24 hours as the Earth rotates. The FUSE orbital inclination is 25°, so the angle between the FUSE orbit normal and the dipole axis varies from 14° to 36° every 24 hours, resulting in significant variations in the pattern of $\vec{\mathbf{B}}$ orientation with orbit phase from one orbit to the next. Finally, the precession of the orbit plane means that $\vec{\mathbf{B}}$-field variations differ from one day to the next.

The limited dipole strength available introduces an additional subtle complication. The A-axis control torque and the S and Z-axis unloading torques may combine to exceed the dipole moment available from one of the torquer bars. In this case the net dipole no longer has the desired orientation, and some of the required A-axis torque is lost. When this occurs, the satellite pointing moves by up to a few degrees for tens of minutes, until the A-axis torque is recovered.

The FUSE Mission Planning team has to evaluate all these varying factors when trying to schedule the roughly 1000 science observations planned for a typical year. When operations in two-wheel mode began in late January 2002, this issue was handled by restricting observations to targets near the orbit pole, where gravity-gradient disturbances are minimized. In the following months sophisticated tools were gradually developed to model all these effects and predict time periods during the year when each target would be accessible. These tools show that most, but not quite all, of the sky is accessible over the course of a year. A plot showing the availability of each region of sky, given present constraints, is given in Reference 3. Three improvements are expected in the near future: some relaxation of the roll-angle requirement (maintaining the sun near the spacecraft X-Z plane), a gradual relaxation of the ram-avoidance constraint as the Earth's upper atmosphere cools following solar maximum, and an improved unloading algorithm that will reduce the competition between the wheel unloading torques and the A-axis control torques when constructing the magnetic dipole with the MTBs. These changes will significantly increase the time available in the regions of the sky that presently have little or no visibility.

Planning slews is even more complex than planning the target pointings. The attitude is of course changing during the slew, hence both the disturbance torque and the available magnetic control torque must be reevaluated throughout the slew. The slew acceleration and deceleration require more torque than static pointing, and the non-zero wheel momenta require allowance for the gyroscopic ($\vec{\omega} \times \vec{\mathbf{L}}$) torques. Slews are presently evaluated manually as a detailed timeline is developed. If a maneuver that is primarily around the A-axis has marginal torque availability, it is usually accomplished instead by a pair of "dogleg" slews rather than a single direct slew to the target. Very long maneuvers are often accomplished by roll-skew-roll combination of slews: an initial roll slew aligns the S axis with the large maneuver, and a final roll slew restores the nominal orientation of the spacecraft axes with respect to the sun after the maneuver.

4. IMPENDING GYRO PROBLEMS

Prior to the unexpected failure of the two reaction wheels, the main concern being addressed by the FUSE project was the impending failure of the ring-laser gyroscopes. The gyroscopes originally supplied by the vendor had shown clear evidence of rapid decline in laser intensity during mission integration and test. An intensive investigation uncovered a process-control problem during manufacture of the lasers; the process was modified and the laser units were rebuilt, requalified, and reinstalled. At the time of launch, the predicted lifetime of the gyroscopes was 5 years. With a backup unit on-board, gyro lifetime was not expected to be a concern. However, in January 2000 both the pitch and yaw axis gyroscopes in IRU A tripped a warning flag which indicated that the laser intensity had dropped to roughly half of the prelaunch value (the intensity measurement itself is not available in telemetry). The roll axis gyro in IRU A tripped its low-intensity warning flag in April 2000, and failed completely on May 30, 2001. The on-board failure detection and correction software switched ACS operations immediately to IRU B, and apart from a few brief periods the satellite has operated exclusively on IRU B since that time.

The first gyro failure occurred after a little more than two years of operation (including prelaunch testing); the remaining life for the other two gyroscopes in IRU A is uncertain. The low-intensity warning flags for two of the three gyroscopes in IRU B tripped relatively quickly: on August 31, 2001 for the pitch axis, and on October 6, 2001 for the roll axis. As of the end of July, 2002, the yaw-axis gyro in IRU B has not tripped its low-intensity warning flag.

Laboratory data indicate that the degradation of laser intensity is roughly exponential with time, until the point at which the discharge is no longer maintained and the laser shuts down. Gyro performance is unaffected by low laser intensity until the laser shuts down; this is ideal from the standpoint of maximizing system performance, but means that there is no advance warning of failure.

Planning for operations without gyroscopes began at a low-level beginning with the first low-intensity warning message in January 2000, but detailed design and analysis work began immediately following the failure of the roll axis gyro. Almost every aspect of the operations flow described above in Section 2.3 has to be redesigned to work in the absence of gyroscopes.

The critical aspects of the redesigned system are as follows:

- Prior to acquisition of guide stars by the FES, attitude drift rates are predicted to be in the range of $10''$/sec to $20''$/sec. This is far higher than the typical rate of $\sim 0.025''$/sec achieved with gyroscopes, and requires that guide stars be located and tracking initiated within 2-3 seconds rather than the 30-60 seconds needed for this process by the original system.

- Once guide stars are acquired in the FES, accurate rate estimation is possible and pointing performance should be similar to what is presently achieved with gyroscopes.

- Because FES data are not available during slews or during occultations of the line of sight by the Earth, a combination of TAM data and a full non-linear model of spacecraft dynamics will be used to estimate angular rates at such times.

- Because TAM data permit attitude determination accurate to better than 1° only for directions perpendicular to the $\vec{\mathbf{B}}$-field, the overall attitude estimate accuracy may be 2° or greater prior to acquisition of FES data.

- Once tracking on guide stars is achieved, the ACS will control to the IDS-supplied attitude estimate rather than its internal attitude estimate, until commanded otherwise by the IDS. This will permit use of FES data to hold a fixed attitude and provide accurate rate information while enough TAM data are accumulated to estimate an accurate 3-axis attitude, which occurs within 2–3 minutes.

- Because the initial attitude uncertainty may be as large as 2°, the star table loaded to the IDS must cover a region roughly 2° in radius, or about 16 times as large an area as that covered by the present star table.

- Two additional types of slews are supported: "dead-reckoning" slews and guided slews. The dead-reckoning slews are used for slew lengths of about $12'$ up to several degrees, and are performed without attitude input from the TAMs. For such short slews the dynamics model will provide greater accuracy than the TAMs (about 10% of the

slew length). These slews will be used for initial attitude correction maneuvers. The guided slews are expected to be used for slew lengths below about $12'$; they are much slower ($<10''$/sec) than normal slews in order to permit tracking of guide stars by the FES during the slew. The guided slews will be used for the final approach to the target. Guided slews require the IDS to select guide stars autonomously from the on-board catalog; for the original system this selection is done manually on the ground.

- Any gyro channels that continue to function will be used for rate measurement.

The region of sky to be covered by the uplinked star catalog for gyroless operations is too large to accommodate simply by scaling the size of the catalog accordingly. The data rate for command uplink would not support such an increase, nor would the execution time of the present star identification algorithm be practical. Instead, several studies were undertaken to improve the present system. A new algorithm was devised to populate the catalog with more uniform spatial sampling and with more stringent criteria on stellar brightness, a new star identification algorithm was developed that executes much faster than the previous algorithm, and the format of the star table was compressed to gain a factor of 6 in required uplink data volume. Finally, the catalog size and the maximum number of stars to be matched from a given FES image were optimized by using a sample of 1120 FES images obtained from acquisitions of 786 different target fields over the past year of operations.

The requirement that guide stars be located and tracking initiated only 2-3 seconds after an FES image is obtained resulted in a substantial modification to the embedded FES software. The limitations on data transfer between the FES and IDS meant that all preliminary processing of the image and selection of stars for centroiding had to be done autonomously by the FES. The FES has an additional new requirement, that it shift the regions of the CCD being read out for centroiding to follow the motion of the guide stars. This is crucial during the initial acquisition when drift rates are high, and during guided slews.

The basic steps in the target acquisition sequence are listed below; they are essentially the same whether following a slew or following emergence from occultation.

1. Begin tracking on unidentified stars with the FES, wait for attitude to stabilize.
2. Wait for the attitude to be determined to better than $2°$ using TAM measurements while holding on guide stars.
3. If the pointing error is worse than $2°$, then:
   (a) The IDS commands ACS to perform a dead-reckoning correction slew to reduce the attitude error.
   (b) The IDS waits for slew to complete and begins again at step 1.
4. Once the pointing error is less than $2°$, the IDS obtains a full FOV image from the FES, and resumes tracking. (Images previously obtained in step 1 may be too smeared by high drift rates to be useful for star identification).
5. The IDS matches objects in the FES image against the star catalog, and determines the absolute attitude.
6. If the attitude error is worse than $12'$, then:
   (a) The IDS commands the ACS to perform a dead-reckoning slew to remove the attitude error.
   (b) The IDS waits for the slew to complete, and starts again at step 1.
7. When the attitude error is less than $12'$, a guided slew to the target is performed, using guide stars selected from the catalog.
8. Proceed with the science observation.

Each dead-reckoning slew is followed by a return to step one because a fast reacquisition of guidestars is required to remove the relatively high angular rates expected to be present. The attitude error will be reevaluated after each slew, and the logic will fall through to the next applicable step.

The new target acquisition sequence will take somewhat longer to execute than the present sequence, although the majority of the visibility period in any given orbit should still remain available for science data acquisition. The main additions to the acquisition duration are as follows:

- The wait in step 2 above for the attitude estimate uncertainty to drop below 2° is likely to be zero as long as one or more gyroscopes are still functioning, and even with no working gyroscopes it is expected to be zero for more than half of the slews. When an additional wait is required, it is expected to be no more than 200-300 seconds. However, if the uncertainty were greater than 2°, then there is a reasonable likelihood that an additional correction slew would be required to reduce the error below 2°; this would add roughly 400 seconds.
- The correction slew in step 6 will be somewhat longer than at present; this will add perhaps 100 seconds to the overall acquisition. If the slew happens to be primarily along the A-axis, the increase in time may be closer to 200 seconds.
- The guided slew in step 7 is a completely new step that may add as much as 120 seconds to the acquisition.
- The new star identification algorithm is much faster than the present algorithm, even though it handles a much larger star catalog, and will save as much as 100 seconds per acquisition.

As can be seen from this discussion, the acquisition duration will be more variable than at present. This will depend primarily on the magnitude of the attitude error at the start of the acquisition, and to a lesser extent on whether or not the direction of the error is predominantly along the A axis.

This target acquisition sequence is more complex than that presently in use, but is actually considerably more robust. The new flight software is more flexible and more capable than the present software, and will be able to handle autonomously the situations that presently require ground intervention. This will provide a significant benefit to overall operating efficiency in the coming extended mission phase of operations, in which staffing levels are reduced and there are fewer real-time contacts with the satellite available for recovery from acquisition failures.

5. SUMMARY

The FUSE attitude control system software is being substantially redesigned to accommodate two significant hardware failures: the loss of two of the four reaction wheels, and the expected eventual loss of the ring-laser gyroscopes. The loss of the reaction wheels required relatively simple changes to the flight software, but substantial new mission planning tools were needed in order to plan observations of targets that are never close to the poles of the orbit. We expect that planned additional refinements will eventually permit access to all regions of the sky, although those that are always far from the orbit poles will be available for fairly limited time intervals over the course of a year. Operating without gyroscopes, however, has necessitated large changes to the software in three flight processors: the Attitude Control System, the Instrument Data System, and the Fine Error Sensor. Conversely, relatively modest changes appear to be required to the mission planning system. The development work needed for gyroless operations is in an advanced state, and is scheduled for implementation early in the Fall of 2002.

ACKNOWLEDGMENTS

The authors would like to thank the FUSE Mission Planning and Mission Operations Teams, and the staff at Orbital Sciences Corp. for their help in this development effort. The new Fine Error Sensor software was contributed by the Canadian Space Agency. The FUSE project at Johns Hopkins University is funded by NASA contract NAS5-32985.

REFERENCES

1. H. W. Moos, W. C. Cash, L. L. Cowie, A. F. Davidsen, A. K. Dupree, P. D. Feldman, S. D. Friedman, J. C. Green, R. F. Green, C. Gry, J. B. Hutchings, E. B. Jenkins, J. L. Linsky, R. F. Malina, A. G. Michalitsianos, B. D. Savage, J. M. Shull, O. H. W. Siegmund, T. P. Snow, G. Sonneborn, A. Vidal-Madjar, A. J. Willis, B. E. Woodgate, D. G. York, T. B. Ake, B.-G. Andersson, J. P. Andrews, R. H. Barkhouser, L. Bianchi, W. P. Blair, K. R. Brownsberger, A. N. Cha, P. Chayer, S. J. Conard, A. W. Fullerton, G. A. Gaines, R. Grange, M. A. Gummin, G. Hebrard, G. A. Kriss, J. W. Kruk, D. Mark, D. K. McCarthy, C. L. Morbey, R. Murowinski, E. M. Murphy, W. R. Oegerle, R. G. Ohl, C. Oliveira, S. N. Osterman, D. J. Sahnow, M. Saisse, K. R. Sembach, H. A. Weaver, B. Y. Welsh, E. Wilkinson, and W. Zheng, "Overview of the Far Ultraviolet Spectroscopic Explorer Mission," *ApJ* **538**, pp. L1–L6, July 2000.

2. D. J. Sahnow, H. W. Moos, T. B. Ake, J. Andersen, B.-G. Andersson, M. Andre, D. Artis, A. F. Berman, W. P. Blair, K. R. Brownsberger, H. M. Calvani, P. Chayer, S. J. Conard, P. D. Feldman, S. D. Friedman, A. W. Fullerton, G. A. Gaines, W. C. Gawne, J. C. Green, M. A. Gummin, T. B. Jennings, J. B. Joyce, M. E. Kaiser, J. W. Kruk, D. J. Lindler, D. Massa, E. M. Murphy, W. R. Oegerle, R. G. Ohl, B. A. Roberts, M. L. Romelfanger, K. C. Roth, R. Sankrit, K. R. Sembach, R. L. Shelton, O. H. W. Siegmund, C. J. Silva, G. Sonneborn, S. R. Vaclavik, H. A. Weaver, and E. Wilkinson, "On-Orbit Performance of the Far Ultraviolet Spectroscopic Explorer Satellite," *ApJ* **538**, pp. L7–L11, July 2000.
3. W. P. Blair, J. W. Kruk, H. W. Moos, and W. R. Oegerle, "Operations with the FUSE Satellite," in *Proc. SPIE Vol. 4854, Future EUV-UV and Visible Space Astrophysics Missions and Instrumentation, J.C. Blades; O. Siegmund; Eds.*, **4854**, Aug. 2002.
4. J. W. Kruk, P. Chayer, J. B. Hutchings, C. L. Morbey, and R. G. Murowinski, "FUSE: fine error sensor optical performance," in *Proc. SPIE Vol. 4139, p. 163-174, Instrumentation for UV/EUV Astronomy and Solar Missions, Silvano Fineschi; Clarence M. Korendyke; Oswald H. Siegmund; Bruce E. Woodgate; Eds.*, **4139**, pp. 163–174, Dec. 2000.
5. B. K. Heggestad and R. C. Moore, "Far Ultraviolet Spectroscopic Explorer (FUSE) Instrument Data System," in *Proc. 18th Digital Avionics Systems Conference (DASC)*, **18**, Oct. 1999.
6. D. A. Artis, L. J. Frank, and B. K. Heggestad, "Scripted Operations in the Far Ultraviolet Spectroscopic Explorer Flight Software," in *Proc. 51st International Astronautical Conference*, **51**, Oct. 2000.
7. T. B. Ake, H. L. Fisher, J. W. Kruk, P. K. Murphy, and W. R. Oegerle, "FUSE attitude control: target recognition and fine guidance performance," in *Proc. SPIE Vol. 4139, p. 175-185, Instrumentation for UV/EUV Astronomy and Solar Missions, Silvano Fineschi; Clarence M. Korendyke; Oswald H. Siegmund; Bruce E. Woodgate; Eds.*, **4139**, pp. 175–185, Dec. 2000.
8. B. Bialke and G. Dorsey, "FUSE Reaction Wheel Torque Anomaly Resolution," in *Proc. 24th Annual Americal Astronautical Society Guidance and Control Conference, R.D. Culp; E.M. Dukes; Eds.*, **107**, pp. 441–450, Jan. 2001.